

R. V. and Lauer H. V. Jr. (1979) *LPSC XX*, 861–863. [11] Morris R. V. et al. (1978) *Proc. LPSC 9th*, 2033–2048. [12] Morris R. V. (1989) *Proc. LPSC 19th*, 269–284. [13] Morris R. V. (1979) *Proc. LPSC 10th*, 1141–1157. [14] Nagle J. S. (1979) *Proc. LPSC 10th*, 1385–1399. [15] Papike J. J. and Wyszynski J. (1980) *Proc. LPSC 11th*, 1609–1621. [16] Rhodes J. M. et al. (1974) *Proc. LSC 5th*, 1097–1117. [17] Ryder G. (1990) *Meteoritics*, 25, 249–258. [18] Salpas P. A. (1987) *Proc. LPSC 17th*, in *JGR*, 92, E340–E348. [19] Simon S. B. et al. (1990) *Proc. LPSC 20th*, 219–230. [20] Stone J. and Clayton R. N. (1989) *Proc. LPSC 19th*, 285–295. [21] Taylor G. J. et al. (1979) *Proc. LPSC 10th*, 1159–1184. [22] Vaniman D. T. et al. (1979) *Proc. LPSC 10th*, 1185–1228. [23] Wentworth S. et al. (1979) *Proc. LPSC 10th*, 207–223. [24] Wolfe E. W. et al. (1981) *U.S. Geol. Surv. Prof. Paper 1080*

N9439/1880004 P-3

GEOCHEMISTRY OF HASP, VLT, AND OTHER GLASSES FROM DOUBLE DRIVE TUBE 79001/2. D. J. Lindstrom¹, S. J. Wentworth², R. R. Martinez², and D. S. McKay¹, ¹NASA Johnson Space Center, Houston TX 77058, USA, ²Lockheed Engineering and Sciences Co., 2400 NASA Road 1, Houston TX 77058, USA.

Background: The Apollo 17 double drive tube 79001/2 (station 9, Van Serg Crater) is distinctive because of its extreme maturity and abundance and variety of glass clasts. It contains mare glasses of both high Ti and very low Ti (VLT) compositions, and highland glasses of all compositions common in lunar regolith samples: highland basalt (feldspathic; $Al_2O_3 > 23$ wt%), KREEP ($Al_2O_3 < 23$ wt%, $K_2O > 0.25$ wt%), and low-K Fra Mauro (LKFM; $Al_2O_3 < 23$ wt%, $K_2O < 0.25$ wt%). It also contains rare specimens of high-alumina, silica-poor (HASP) and ultra Mg' glasses. HASP glasses [1] contain insufficient SiO_2 to permit the calculation of a standard norm, and are thought to

TABLE 1. Average compositions of common glass types in 79002.

(Wt%)	n=	H B	LKFM	VLT5	VLT6	High Ti
		5	23	7	21	16
SiO ₂		44.65	46.76	46.80	46.39	38.73
TiO ₂		0.24	1.15	0.86	0.87	8.87
Al ₂ O ₃		26.31	19.00	10.83	12.25	6.00
Cr ₂ O ₃		0.11	0.24	0.62	0.52	0.66
FeO		4.25	9.27	17.13	17.65	22.37
MnO		0.06	0.13	0.25	0.27	0.27
MgO		8.43	10.35	12.05	10.54	13.90
CaO		15.37	12.15	9.85	10.67	7.50
Na ₂ O		0.12	0.41	0.19	0.16	0.43
K ₂ O		0.03	0.11	0.06	0.02	0.10
P ₂ O ₅		0.02	0.05	0.05	0.03	0.06
Total		99.62	99.67	98.71	99.39	98.98
CaO/Al ₂ O ₃		0.58	0.64	0.92	0.87	1.27
Mg/Mg + Fe		0.77	0.67	0.56	0.52	0.52
(μg/g)	n=	4	7	4	7	2
Sc		8	21	55	55	49
Cr		740	1650	5050	3430	4450
Co		10	25	46	21	62
La		4	4–45	1.1	2.5	6.0
Sm		1.7	2–20	0.9	1.6	6.4
Yb		1.6	1.8–16	1.4	2	4.3

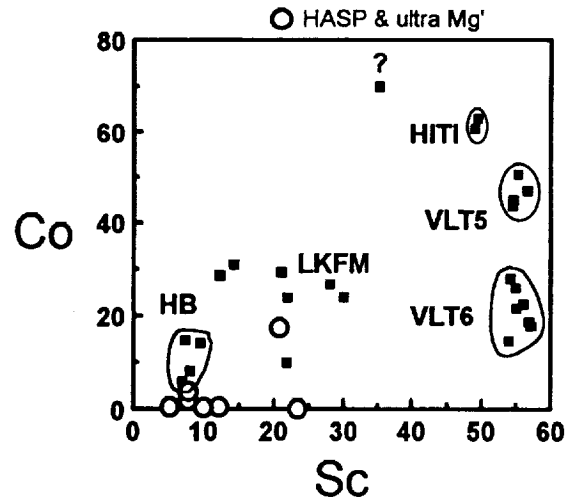


Fig. 1.

be the product of volatilization during impact melting. They have been studied by electron microprobe major-element analysis techniques but have not previously been analyzed for trace elements.

Samples and Methods: The samples analyzed for this study were polished grain mounts of the 90–150-μm fraction of four sieved samples from the 79001/2 core (depth range 2.3–11.5 cm). 80 glasses were analyzed by SEM/EDS and electron microprobe, and a subset of 33 of the glasses, representing a wide range of compositional types, was chosen for high-sensitivity INAA [2]. A microdrilling device removed disks (mostly 50–100 μm diameter, weighing ~0.1–0.5 μg) for INAA. Preliminary data reported here are based only on short counts done within two weeks of irradiation.

Results: Almost half the 80 glasses analyzed by electron microprobe are highland compositions, mostly with compositions ranging from LKFM to KREEP. Seven LKFM glasses were shown by INAA to have typically moderate Sc, Cr, and Co contents and a considerable range in REE (Table 1), and are not discussed further here. Of the more interesting 13 highland samples, five samples are classed as highland basalts. Six samples have HASP compositions (Table 2),

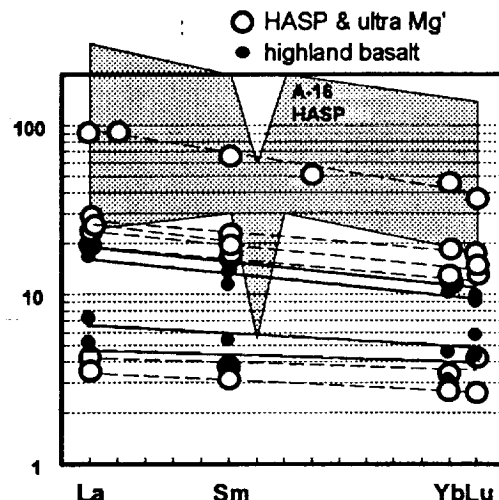


Fig. 2.

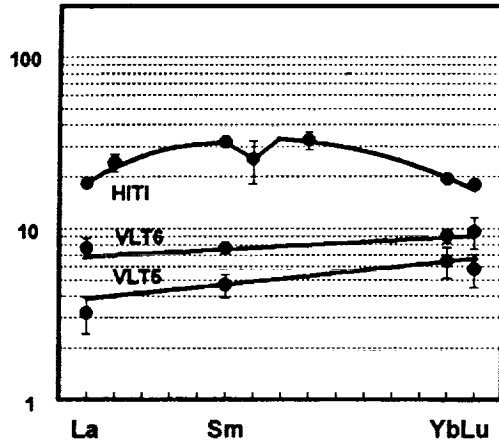


Fig. 3.

and four of the six also fall into the ultra Mg' (atomic Mg/Mg + Fe > 0.90) category. Two HASP glasses have more normal Mg' values, while two additional glasses have non-HASP, ultra Mg' compositions. INAA trace-element results on these 13 particles do not correlate strongly with the major element categories. Most of these glasses are low in ferromagnesian elements (Tables 1 and 2, Fig. 1), and all but one (,146-10) have REE contents below the range observed by [3] in Apollo 16 ultra Mg' glasses (Fig. 2). Except for ,146-10, the REE patterns appear to form two groups, those with 3-7 \times chondritic La and those with 16-30 \times . Whether the gap between

them is real or merely due to the small numbers of samples analyzed is not clear. The important point is that ultra Mg' and HASP samples occur in both groups, as do highland basalts, which are the best candidates for precursors of most of these HASP and ultra Mg' glasses.

Mare glasses comprise the other half of the samples microprobed. Sixteen of these have high-Ti compositions, and just two of them were analyzed by INAA, showing the typical bow-shaped REE patterns (Fig. 3). VLT glasses were more numerous and included 6 VLT5 and 21 VLT6 glasses (the "mare 5" and "mare 6" varieties of [4]). These glasses form tight compositional groups, with a clear separation between the two groups in both major- and trace-element data. The VLT5 group glasses contain almost twice the Co, higher MgO, lower Al₂O₃, and about 1.5 \times lower REE than the VLT6 group. Previous analyses of Apollo 17 VLT lithic clasts [5] found only the VLT5 trace-element pattern. The VLT6 glasses cluster very tightly compositionally (e.g., 21 analyses for Al₂O₃ ranged from 12.01% to 12.67%), suggesting that this may be a pyroclastic deposit.

Conclusions: Much can be learned from small glass samples by first using SEM/microprobe analyses of grain mounts to scan a large number of particles to find those with interesting compositions, then microdrilling to obtain samples for high-sensitivity INAA for trace elements. This technique has shown that five out of seven of the HASP and ultra Mg' glasses found in these 79002 soils are most likely to be formed from the highland basalts. While cobalt follows iron in being lost, presumably due to the extreme impact heating that produces these glasses, characteristic abundances of Sc, Cr, REE, and other refractory elements remain in the melt. These five glasses are all quite low in REE and Sc, and most closely resemble the noritic anorthosite composition of some of the lunar meteorites [e.g., 6].

TABLE 2. Compositions of HASP and ultra Mg' glasses in 79002.

(Wt%)	Ultra Mg HASP				Non-HASP Ultra Mg		Other HASP	
	,143 23	,143 33	,145 25	,146 33	,146 4	,146 10	,142 16	,143 31
SiO ₂	43.01	41.21	40.68	36.29	43.03	52.41	37.64	40.23
TiO ₂	0.28	0.23	0.23	0.23	0.21	1.50	1.30	0.38
Al ₂ O ₃	28.76	29.39	34.06	32.85	32.17	20.14	25.69	27.84
Cr ₂ O ₃	0.15	0.12	0.05	0.09	0.08	0.24	0.10	0.13
FeO	1.09	2.03	0.65	0.68	0.62	1.95	7.88	4.46
MnO	0.03	0.04	0.01	0.01	0.00	0.16	0.11	0.07
MgO	10.50	11.15	3.91	11.06	4.08	9.64	10.76	10.71
CaO	16.18	16.06	20.23	18.17	18.81	12.85	15.63	16.70
Na ₂ O	0.12	0.01	0.01	0.01	0.01	0.24	0.01	0.04
K ₂ O	0.01	0.01	0.00	0.00	0.01	0.12	0.00	0.01
P ₂ O ₅	0.04	0.03	0.00	0.01	0.00	0.01	0.01	0.03
Total	100.27	100.28	99.85	99.42	99.01	99.31	99.16	100.60
CaO/Al ₂ O ₃	0.56	0.55	0.59	0.55	0.58	0.64	0.61	0.60
Mg/Mg Fe	0.95	0.91	0.91	0.97	0.92	0.90	0.71	0.81
Sc	8	8	12	—	10	23	21	5
Cr	870	890	460	—	650	1400	750	360
Co	2	3	<2	—	<2	<4	17	<12
La	8	7	1.4	—	1.2	29	9	6
Sm	3.3	2.9	0.8	—	0.6	13	4.6	2.9
Yb	2.8	2.5	0.8	—	0.6	10	4.0	<5

References: [1] Nancy M. D. et al. (1976) *Proc. LSC 7th*, 155-184. [2] Lindstrom D. J. (1990) *Nucl. Instr. Meth. Phys. Res.*, A299, 584-588. [3] Shearer C. K. et al. (1990) *GCA*, 54, 1851-1857. [4] Warner R. D. et al. (1979) *Proc. LPSC 10th*, 1437-1456. [5] Wentworth S. J. et al. (1979) *Proc. LPSC 10th*, 207-233. [6] Lindstrom M. M. et al. (1991) *GCA*, 55, 3089-3103.

P. 1 N 93-1880 B05
THE TAURUS-LITTRAW DARK MANTLE, LIGHT MANTLE, CRATER CLUSTER, AND SCARP. Baerbel K. Lucchitta, U.S. Geological Survey, Flagstaff AZ 86001, USA.

The Taurus-Littrow landing site is on the floor of a grabenlike valley that is radial to the Serenitatis Basin; the valley is gently inclined to the east. It is bordered by steep-sided massifs that rise 2 km above the valley floor and form part of the Serenitatis Basin rim [1,2]. The valley floor is exceptionally dark, and in one place it is overlain by a light-colored mantle apparently derived from the massif to the south. The floor is also peppered by overlapping craters. A scarp, up on the west, transects the valley floor and enters the highlands to the north.

Before the mission, the valley floor was interpreted to be covered by a dark mantle that also covers part of the highlands along the southeastern rim of the Serenitatis Basin [3-5]. The dark unit has an albedo as low as 0.79, which is darker than the outer dark mare ring in the Serenitatis Basin [6]. The dark mantle was generally interpreted to be a young pyroclastic deposit. The reasons for the young age assignment were (1) a dearth of small craters when compared with crater densities on surrounding mare surfaces and (2) the observation that the dark mantle appears to cover young craters and the fresh-looking scarp. Postmission analysis established that the dark material in the landing area is mostly composed of old mare regolith averaging about 14 m in thickness and containing about 5% dark beads [7]. These beads are associated with orange beads in the ejecta of a small crater. The generally accepted postmission interpretation of the dark mantle is that it is a deposit of dark and orange beads erupted from fire fountains soon after the mare basalts were emplaced [7], and that the reworking of the beads into the regolith gave it the low albedo [1,2]. The presence of orange and dark layers on mare and highland material at the base of the regolith is also supported by detailed studies of the Sulpicius Gallus Formation on the west side of the Serenitatis Basin, where many outcrops give clues to the stratigraphic relations [8]. There the dark mantle covers mare and highlands with deposits on the order of 50 m thick. The reason for the paucity of small craters in the dark mantle is now attributed to the unconsolidated, friable nature of the mantle; small craters are eroded much more rapidly by mass wasting and impact gardening than in the adjacent hard-surfaced, younger lavas, which have thin regoliths [9].

The controversy concerning the light mantle mostly centers on whether it is a simple avalanche deposit or whether it was emplaced largely by impact (whereby secondary projectiles may have hit the top of the massif from which the light mantle is derived and dislodged the material). A detailed study of secondary impact craters of Tycho over the entire lunar nearside showed that Tycho secondaries have distinctive characteristics [10]: they are crater clusters with sharp, fresh-looking surface textures; the surface downrange from secondary craters displays a braided pattern with V-shaped grooves and ridges; acute angles of the Vs as well as the trend of many ridges, together with the overall cluster trend, point in the general direction of Tycho. An analysis of the light mantle, the crater cluster on top of the massif, and the crater cluster on the valley floor showed that the Tycho secondary characteristics are present. Thus, the light mantle is not a

true avalanche but an impact-propelled feature, and the crater cluster on the valley floor is composed of Tycho secondaries. The scarp on the valley floor displays the typical characteristics of a mare-type wrinkle ridge. Wrinkle ridges in the Serenitatis region were studied by several authors [11] and were generally considered to be thrust faults. A detailed study of the scarp on the valley floor and its continuation into the adjacent highlands showed that it has characteristics of high-angle normal and high-angle reverse faults [12]. It is likely that this scarp is the surface expression of minor postmare adjustments along high-angle faults that reactivated older faults bordering basin-rim massifs.

References: [1] Wolfe E. W. et al. (1975) *Proc. LSC 6th*, 2463-2482. [2] Wolfe E. W. et al. (1981) *U.S. Geol. Surv. Prof. Paper 1080*, 280 pp. [3] Scott D. H. and Carr M. H. (1972) *U.S. Geol. Surv. Misc. Geol. Inv. Map I-800*, sheet 1. [4] Lucchitta B. K. (1972) *U.S. Geol. Surv. Misc. Geol. Inv. Map I-800*, sheet 2. [5] Lucchitta B. K. (1973) *Proc. LSC 4th*, 149-162. [6] Pohn H. A. and Wilkey R. L. (1970) *U.S. Geol. Surv. Prof. Paper 559-E*, 20 pp. [7] Heiken G. H. et al. (1974) *GCA*, 38, 1703-1718. [8] Lucchitta B. K. and Schmitt H. H. (1974) *Proc. LSC 5th*, 223-234. [9] Lucchitta B. K. and Sanchez A.G. (1975) *Proc. LSC 6th*, 2427-2441. [10] Lucchitta B. K. (1977) *Icarus*, 30, 80-96. [11] Muehlberger W. R. (1974) *Proc. LSC 5th*, 101-110. [12] Lucchitta B. K. (1976) *Proc. LSC 7th*, 2761-1782.

N 93-188023 06 P. 6
MORPHOLOGY AND COMPOSITION OF CONDENSATES ON APOLLO 17 ORANGE AND BLACK GLASS. David S. McKay¹ and Sue J. Wentworth², ¹NASA Johnson Space Center, Houston TX 77058, USA, ²Lockheed, 2400 NASA Road 1, Houston TX 77058, USA.

Background: Lunar soil sample 74220 and core samples 74001/2 consist mainly of orange glass droplets, droplet fragments, and their crystallized equivalents. These samples are now generally accepted to be pyroclastic ejecta from early lunar volcanic eruptions [1,2]. It has been known since early examination of these samples that they contain surface coatings and material rich in volatile condensable phases, including S, Zn, F, Cl, and many volatile metals. Meyer [3] summarizes the voluminous published chemical data and calculates the volatile enrichment ratios for most of the surface condensates.

The volatiles associated with these orange and black glasses (and the Apollo 15 green glasses) may provide important clues in understanding the differentiation and volcanic history of the Moon. In addition, condensable volatiles can be mobilized and concentrated by volcanic processes.

The Problem: While considerable chemical data exist on these samples, the phases that contain the volatile species are not known; no unequivocal condensate mineral has ever been identified in these samples, with the possible exception of sodium chloride salt crystals [4]. No X-ray diffraction or electron diffraction data exist on any of these phases. More positive information on the phases or mineralogy of the condensates would lead to a better understanding of the nature of the volatile gases from which they formed and the temperature, total pressure, and gas fugacity conditions associated with the eruption. This in turn would lead to a better understanding of lunar extrusive volcanism and of the history of the magma from which the pyroclastics came.

Some basic questions still unanswered include

1. What is the composition of the gas phase of the eruption? Was the major driving gas CO-CO₂ or was it something else?
2. What is the source of the condensable volatiles found on the droplets? Are they all indigenous lunar volatiles? Are any of them,